

Risk of COVID-19 epidemic resurgence with the introduction of vaccination passes

Tyll Krueger^{1,*}, Krzysztof Gogolewski^{2,*}, Marcin Bodych^{1,*}, Anna Gambin², Giulia Giordano³, Sarah Cuschieri⁴, Thomas Czypionka^{5,6}, Matjaz Perc^{7,8,9,10}, Elena Petelos^{11,12}, Magdalena Rosińska¹³, and Ewa Szczurek^{2,†}

¹*Faculty of Electronics, Department of Control Systems and Mechatronics, Wrocław University of Science and Technology, Wrocław, Poland*

²*Faculty of Mathematics, Informatics and Mechanics, University of Warsaw, Warszawa, Poland*

³*Department of Industrial Engineering, University of Trento, Trento, Italy*

⁴*Department of Anatomy, Faculty of Medicine and Surgery, University of Malta, Msida, Malta*

⁵*Institute for Advanced Studies, Josefstädterstraße 39, 1080, Vienna, Austria*

⁶*London School of Economics and Political Science, Houghton Street, WC2A 2AE, London, UK.*

⁷*Faculty of Natural Sciences and Mathematics, University of Maribor, Koroška cesta 160, 2000 Maribor, Slovenia*

⁸*Complexity Science Hub Vienna, Josefstädterstraße 39, 1080 Vienna, Austria*

⁹*Department of Medical Research, China Medical University Hospital, China Medical University, Taichung 404332, Taiwan*

¹⁰*Alma Mater Europaea, Slovenska ulica 17, 2000 Maribor, Slovenia*

¹¹*Clinic of Social and Family Medicine, Faculty of Medicine, University of Crete, Heraklion, Greece.*

¹²*Department of Health Services Research, CAPHRI-Care and Public Health Research Institute, Maastricht University, Maastricht, The Netherlands*

¹³*Department of Infectious Disease Epidemiology and Surveillance, National Institute of Public Health, Warsaw, Poland.*

**Shared first authorship*

†*Correspondence: szczurek@mimuw.edu.pl*

23 **Many countries hit by the COVID-19 epidemic consider the introduction of vaccina-**
24 **tion passes. So far, no thorough impact assessment of vaccination passes and of lower**
25 **restrictions for their holders has been conducted. Here, we propose the VAP-SIRS model**
26 **that accounts for susceptible, infected, and recovered subpopulations, also within the**
27 **group of vaccinated pass holders. The model accounts for imperfect vaccination effec-**
28 **tiveness, revaccinations and waning immunity. Different restrictions for pass holders and**
29 **the rest of the population result in different scenarios of the epidemic evolution, some of**
30 **which yield unfavourable COVID-19 dynamics and new waves. We identify critical vari-**
31 **ables that should be considered by policymakers and show how unfavourable outcomes**
32 **can be avoided using adaptive policies. In particular, while pass holders could initially be**
33 **allowed large freedoms, the gradual loss of immunity will require either increased restric-**
34 **tions for pass holders, or accelerated revaccination. In the long-term, common restrictions**
35 **for both the pass holders and the rest of the population will have to be kept to avoid epi-**
36 **demic resurgence. Such minimum required restrictions depend on vaccination effective-**
37 **ness, revaccination rate, waning rate and fraction of never-vaccinated population, and,**
38 **for realistic combinations of these parameters, range between 29% and 69% reduction of**
39 **contacts.**

40 **Main**

41 In the past, governments have required proof of vaccination for travel, with yellow fever being
42 the best-known example, and the only disease for which a certificate is needed to cross borders
43 in compliance to the International Health Regulations¹. However, the idea that proof of vac-
44 cination will become a prerequisite for crossing borders or to enter facilities, visit businesses
45 premises, participate in events, and generally enjoy more freedom, has only arisen in the context
46 of combatting the COVID-19 epidemic. Despite technical challenges, scientific uncertainties,
47 and ethical and legal dilemmas, the idea of vaccination passes (VPs), i.e., documents issued on
48 the basis of vaccination status, is now receiving unprecedented attention^{2,3,4}. Many consider
49 VPs as tools to restore people's freedoms and increase well-being, whilst allowing economies
50 to reopen. Determining immunity status is challenging, as the immune response and its dura-

51 tion may greatly vary; this being applicable to post-vaccination immunity, as well as following
52 natural SARS-CoV-2 infection and recovery⁵. It is, therefore, critically important to determine
53 levels of restrictions that offer safety whilst being tolerable, ensuring good compliance and
54 rational behaviour. Less than perfect conferred protection coupled with suboptimal levels of
55 restrictions can have detrimental effects. The lack of a comprehensive framework to determine
56 such levels, including when approaching higher vaccination coverage and even herd immunity,
57 may result in policymakers opting to select suboptimal levels of restrictions. This may happen
58 for different reasons, such as lack of true understanding of the ramifications, to boost morale or,
59 even, for political gain. Evidence indicates vaccine effectiveness can greatly vary^{6,7} and it may
60 be compromised due to escape variants⁸ and waning immunity^{9,10,11,12}.

61 Various models have been developed to inform vaccination strategies^{13,14,15,16,17,18,19,20,21}.
62 One such effort indicates lower vaccine effectiveness coupled with an increase in social con-
63 tact among those vaccinated (behavioral compensation) may undermine vaccination effects,
64 even without considering immunity waning²². So far, there has been no model to focus on the
65 medium- and long-term impact of relaxing restrictions for VP holders, with due consideration to
66 vaccine effectiveness, durability of response, and vaccine hesitancy. The proposed VAP-SIRS
67 model delivers a systematic framework to assess key considerations for policymaking.

68 **Results**

69 **The VAP-SIRS model of the impact of COVID-19 vaccination passes**

70 The VAP-SIRS model extends the classical SIRS model²³ (red arrows in Fig. 1a) with addi-
71 tional states and parameters that describe the dynamics of vaccination routine in a population
72 (green arrows in Fig 1a.). To this end, we consider the following subpopulations: (i) initially
73 susceptible S_N , who, if successfully vaccinated, populate the immune group V , with rate av ,
74 where v is the vaccination rate and a is the effectiveness, (ii) susceptible who were vaccinated
75 but did not gain immunity (S_1), (iii) vaccinated, whose immunity waned with rate ω and be-
76 came susceptible again (S_2), (iv) susceptible, who are not and will never get vaccinated (S_D).
77 Additionally, revaccination of S_2 populates V with rate av_r . All recovered, unless recovered

78 compartment R_D , are also subject to vaccination. The fraction of the population that will never
79 be vaccinated is denoted d .

80 The presented model analysis is performed for carefully selected parameter setups: two
81 different vaccination rates, 0.004 and 0.008 dose per person daily, chosen on the basis of the
82 current rates observed in Europe^{24,25}, and for vaccine effectivenesses 0.6 and 0.9, which conser-
83 vatively model that of the most widely used vaccines: Vaxzevria (AstraZeneca)^{26,27} and Comir-
84 naty (BioNTech/Pfizer)^{28,7,29}, respectively. Furthermore, optimistic (500 days; $\omega = 1/500$)
85 and pessimistic (200 days; $\omega = 1/200$) average immunity duration periods are considered, re-
86 flecting emerging data on large individual variation of immunity waning and other key factors
87 influencing this process^{9,12,30,31,32}. Finally, across the manuscript, we assume the revaccination
88 rate $v_r = v$, and consider optimistic 0.1, and pessimistic 0.3 fractions of never-vaccinated d .

89 We assume that VP holders are all who were vaccinated at least once (Fig. 1). The restriction
90 level f (ranging from 0 to 1) is introduced as a modulator of the SARS-CoV-2 reproduction
91 number. Here, we consider that without any restrictions ($f = 0$), the reproduction number for
92 the virus equals 4, as an optimistic estimate for B.1.1.7^{33,34}. Similarly, restrictions $f_v \leq f$ for
93 contacts among VP holders are considered. f and f_v should be interpreted as the net effect
94 of all factors that reduce the reproduction number of the virus within the respective groups:
95 all applied non-pharmaceutical interventions together with the resulting changes in behavior.
96 Based on the current studies, we fix the generation time to 6 days ($\gamma = 1/6$)^{34,33}. Finally, we
97 consider two types of mixing between subpopulations: proportional (typical for SIR models)
98 and preferential, where the VP holders prefer contacts with other VP holders. See Methods for
99 a detailed model description.

100 **VAP-SIRS predicts a possible infection resurgence despite vaccinations**

101 VAP-SIRS predicts unfavourable epidemic dynamics for a wide range of parameters. As an
102 example consider: $a = 0.9$, $v = v_r = 0.004$, $d = 0.1$, and $\omega = 1/500$, a seemingly safe
103 setup, which we will call the reference setup. For such setup and low restrictions $f_v = 0.05$
104 for VP holders as well as medium restrictions $f = 0.63$ for contacts with and within the rest
105 of the population, the model predicts a small wave of infections shortly after the vaccination

106 program starts, followed by a large wave later (Fig. 1b). This behavior is explained by the
 107 population structure and different restrictions (Fig. 1c). In this scenario, the first wave is driven
 108 by the unvaccinated susceptibles (S_N) and suppressed by ongoing vaccination, as expected.
 109 Interestingly, the second, larger wave is driven by the S_V group. The S_V group is composed of
 110 the number of individuals for whom the vaccine was ineffective (S_1) and those vaccinated who
 111 lose their immunity and are not yet revaccinated (S_2). In the following we investigate how the
 112 dynamics change for different restrictions settings.

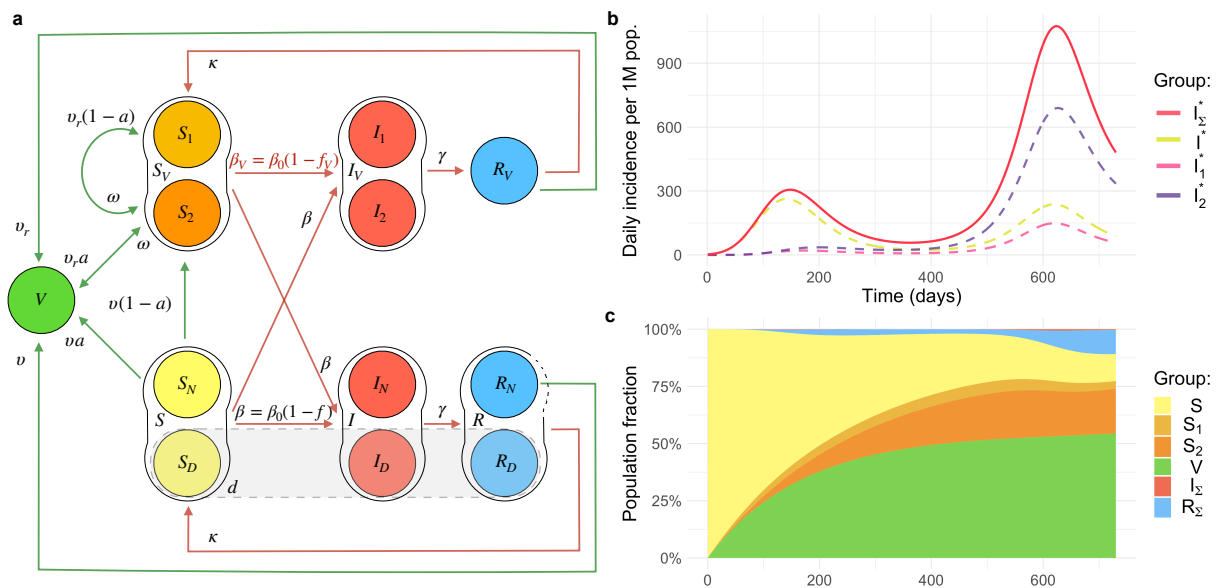


Figure 1: **The VAP-SIRS model shows the possible rebound of infections after a large population is vaccinated and obtains a VP, but then loses immunity.** **a.** Graphical scheme of the VAP-SIRS model. **b.** The timeline of daily incidence per 1 million inhabitants for an effective vaccine ($a = 0.9$), slow (re-)vaccination rate ($v = v_r = 0.004$; typical for many European countries), proportional mixing (see Methods) and low fraction of never-vaccinated ($d = 0.1$). Here, a variable with the asterisk (*) indicates that we consider a daily incidence over the corresponding variable, thus I^* stands for $I_D^* + I_N^*$, and by I_Σ^* we mean the sum of all daily infected ($I^* + I_1^* + I_2^*$). **c.** The Muller plot of the population structure (the width of the color band in the y axis) as a function of time (x axis) for the same parameter settings as in **b.** Here, by I_Σ and R_Σ we denote $I + I_V$ and $R + R_V$, respectively.

113 **Stability analysis identifies potential scenarios for the COVID-19 epidemic**
114 **depending on the restrictions imposed on VP holders and the rest of the**
115 **population.**

116 To assess the epidemic evolution in different scenarios, we analysed stability by linearising the
117 model equations with $I = R = 0$ (Methods). The restriction levels $\mathbf{f} = (f, f_v)$ influence
118 the *instantaneous reproduction number* R^* . $R^*(t)$ is the reproduction number that would be
119 observed at time t , given the restrictions \mathbf{f} and the composition of the population, where the
120 number of infected is very small. If $R^*(t) > 1$, then switching to \mathbf{f} at time t results in an
121 *overcritical* epidemic evolution, with an initially exponential growth of infections; if $R^*(t) < 1$,
122 switching to \mathbf{f} at time t results in a *subcritical* epidemic evolution, where the number of active
123 cases decreases to zero. The R^* is more informative of epidemic thresholds than the standard
124 effective reproduction number, as it does not depend on the actual number of infected and
125 recovered.

126 We consider five restriction choices (prototypical for five regions of the parameter space),
127 leading to different time profiles of R^* (Fig. 2a). Medium restrictions for both VP holders
128 and the rest of the population (red curve in Fig. 2a) lead to an overcritical epidemic. Medium
129 restrictions for VP holders and strong restrictions for the others (blue curve in Fig. 2a) lead to
130 a subcritical epidemic. With low restrictions for VP holders and medium restrictions for the
131 rest of the population (orange curve in Fig. 2a), the epidemic is initially overcritical, becomes
132 subcritical and then switches to overcritical again; this is the scenario shown in the simulation
133 in Fig. 1b,c. With very low restrictions for VP holders and strong restrictions for the rest of
134 the population (pink curve in Fig. 2a), the epidemic is initially subcritical and then becomes
135 overcritical. If low restrictions are adopted for VP holders and medium restrictions for the rest
136 of the population (cyan curve in Fig. 2a), the epidemic is initially overcritical and then switches
137 to subcritical.

138 In each scenario we computed the time evolution of the *instantaneous doubling time* D
139 (Methods). For a given \mathbf{f} , $D(t)$ is the doubling time (capturing how fast the infections grow)
140 that would be observed for the growth of a small initial number of infections at time t , with

141 enforced restrictions f . Very short doubling times, below 30 days, can be observed in three
 142 scenarios that are (eventually) overcritical: see the red, orange and pink curves in Fig. 2b.

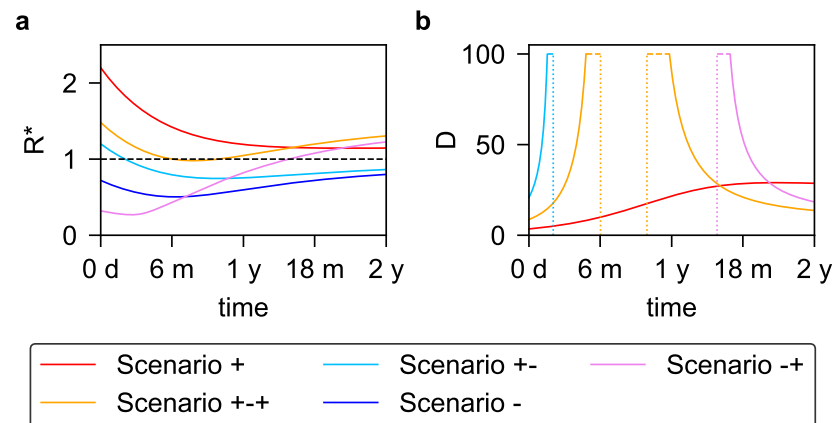


Figure 2: **Intensity and timing of the infection wave: examples of five scenarios depending on the restrictions for VP holders and for the rest of the population.** Given $a = 0.9$, $v = v_r = 0.004$, $\omega = 0.002$, $d = 0.1$ and proportional mixing, we compare five different scenarios describing the epidemic evolution: overcritical (+, red, $f = 0.45$ and $f_v = 0.32$), subcritical (-, blue, $f = 0.82$ and $f_v = 0.4$), initially and eventually overcritical (+-+, orange, $f = 0.63$ and $f_v = 0.05$), eventually overcritical (-+, pink, $f = 0.92$ and $f_v = 0.04$), eventually subcritical (+-, cyan, with $f = 0.7$ and $f_v = 0.4$). **a.** Time evolution of R^* (y axis) depending on the number of days counted from the start of the vaccination program (x axis). **b.** Doubling time D (y axis, in days) as a function of the number of days (x axis). Note that doubling curves are cut above 100 days, in the time intervals indicated by the horizontal dashed lines. Negative doubling times (halving times) are not plotted. Thus, the subcritical scenario (-) is not visualised in **b.** Vertical dotted lines indicate the times at which a transition occurs from overcritical to subcritical, or vice versa.

143 **Different restrictions are required to avoid epidemic resurgence depending**
 144 **on parameter setups**

145 The relevant $f - f_v$ parameter space, where $f_v \leq f$, can be divided into five regions, where the
 146 epidemic dynamics follows the distinct patterns exemplified in Figure 2. The area occupied by
 147 each region changes depending on the parameter setups, as shown in Figure 3. For example,
 148 in the reference setup in Figure 3a (high vaccine effectiveness $a = 0.9$ and (re-)vaccination
 149 rates $v = v_r = 0.004$, low never-vaccinated fraction $d = 0.1$ and low immunity waning rate
 150 $\omega = 0.002$), the overcritical region (with R^* always above 1) occupies the lower left corner. It
 151 is enlarged with smaller vaccine effectiveness ($a = 0.6$, Fig. 3b), larger fraction of the never-

152 vaccinated population (Fig. 3e) and higher waning rate (Fig. 3f), while it shrinks with higher
153 vaccination rate (Fig. 3c). The subcritical region - (with R^* always smaller than 1) lies in
154 the opposite corner of the $f - f_v$ space, for larger values, and for a fixed fraction of never-
155 vaccinated d tends to decrease for setups where the overcritical region increases. Inside each of
156 the remaining three regions (associated with the $++$, $-+$, $+ -$ scenarios in Figure 2), the specific
157 parameter settings differ by the time to the critical threshold of interest for that region (the last
158 observed switch between subcritical and overcritical epidemic, which for the $++$ region, for
159 example, is the second critical threshold; see Methods for the computation of the times to critical
160 thresholds). For the reference setup (Fig. 3a), the critical threshold is reached after a minimum
161 ~ 8 months. Decreasing vaccine effectiveness (Fig. 3b), as well as increasing the waning rate
162 (Fig. 3f), enlarges the $++$ region' and leads to overcriticality sooner, after ~ 3 and ~ 4 months
163 respectively, for low f_v values. Increasing vaccination rate (Fig. 3c) shrinks the $++$ region.
164 With preferential mixing (Fig. 3d), the $++$ region becomes larger and overcriticality is reached
165 even sooner. Increasing the number of never-vaccinated people (Fig. 3e) shrinks the $++$ region
166 and delays the onset of overcriticality. For all considered parameter setups, except for the one
167 with high (re-)vaccination rate, for all except the $+ -$ and the $-$ regions, large asymptotic R^* can
168 be expected, which corresponds to short doubling times (Fig. 3).

169 These results indicate that VP holders can be granted large freedom, as long as sufficient
170 restrictions are enforced for the rest of the population, to avoid an initially overcritical situation.
171 However, to prevent the epidemic from becoming overcritical after an initial decline in case
172 numbers, restrictions on VP holders need to be timely increased and adapted so that eventually
173 everyone faces the same restrictions. Safe restrictions correspond to the parameters in the sub-
174 critical region, but these are relatively high and could be unacceptable for the population. The
175 $-+$ and $++$ regions can seem attractive from the aspect of large freedom for the VP holders.
176 Both these regions, however, eventually result in epidemic resurgence and should be avoided.
177 Moving to the $+ -$ region with the right timing is a recommendable strategy.

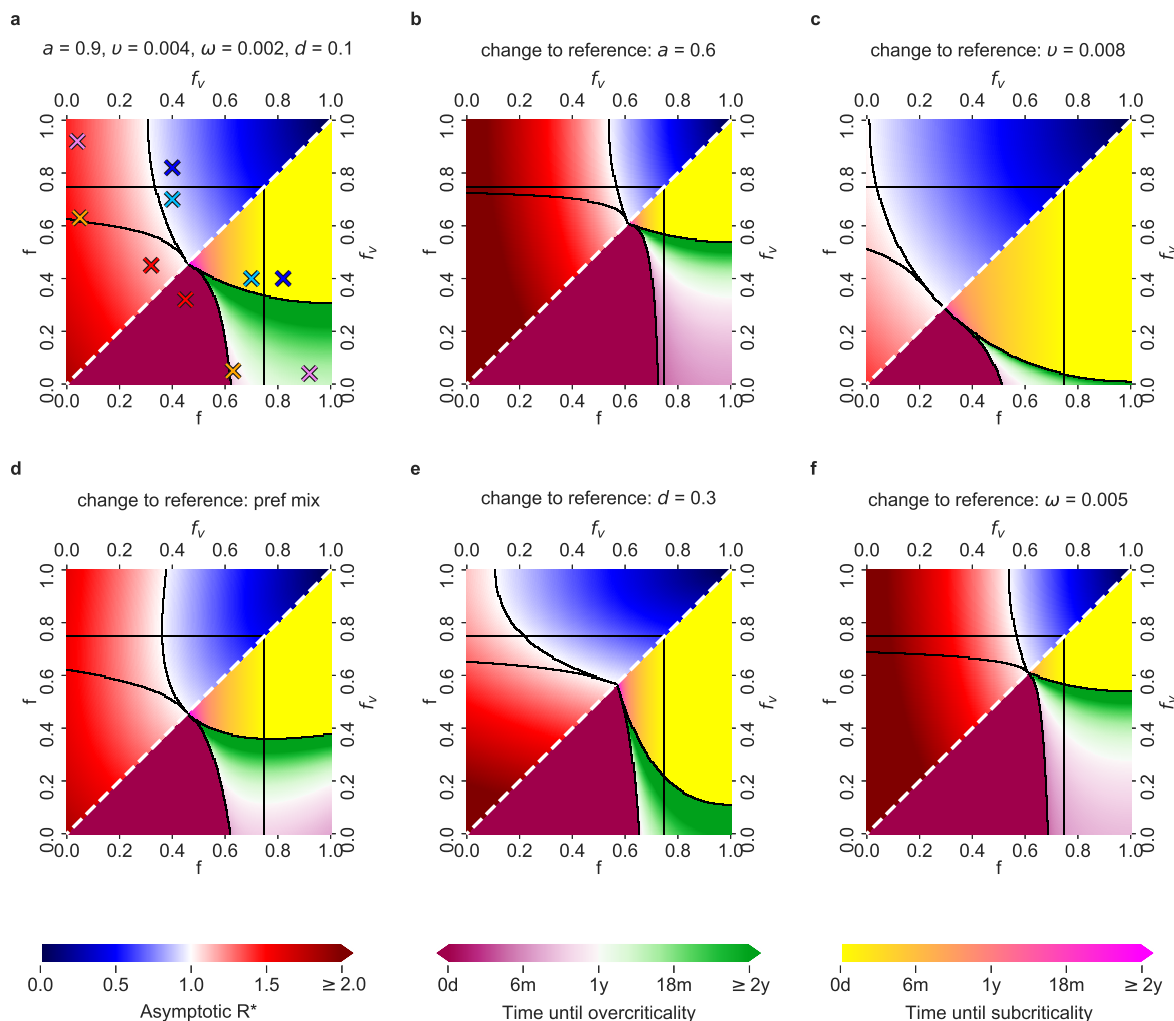


Figure 3: Possible COVID-19 epidemic dynamics depending on vaccine effectiveness, vaccination rate, mixing type and the restrictions for VP holders and for the rest of the population. For various choices of the other parameters, the relevant $f - f_v$ parameter space, where $f_v \leq f$, can be divided into five regions, each associated with a different behavior of the epidemic, exemplified by the five scenarios in Figure 2a. On the diagonal (white dashed line), $f = f_v$, namely the restrictions for VP holders and for the rest of the population are the same. Lower triangles show the time until the last critical threshold: different colour scales correspond to the time until the switch either from a subcritical to an overcritical epidemic (time until overcriticality, violet-green scale), or from an overcritical to a subcritical epidemic (time until subcriticality, yellow-pink scale). Upper triangles show the asymptotic R^* , as a function of the values of f and f_v (blue-red scale, with blue associated with $R^* < 1$ and red associated with $R^* > 1$). **a.** Reference setup, with $a = 0.9$, $v = v_r = 0.004$, $\omega = 0.002$, $d = 0.1$ and proportional mixing. The choices of (f, f_v) corresponding to the five scenarios exemplified in Figure 2 are denoted by crosses of the same colour. **b.** Setup with decreased vaccine effectiveness: $a = 0.6$. **c.** Setup with increased vaccination rate: $v = v_r = 0.008$. **d.** Setup with preferential (instead of proportional) mixing. **e.** Setup with increased fraction of people who will not get vaccinated: $d = 0.3$. **f.** Setup with increased waning rate: $\omega = 0.005$.

178 **A minimum common restriction level is required to keep the epidemic sub-** 179 **critical**

180 We compute the minimum common restriction level f_{\min} for the whole population that would
181 be required to avoid an overcritical epidemic in the long-term (Methods):

$$f_{\min} = \max(0, 1 - 1/(4 \cdot (1 - V^{\text{as}}))),$$

182 where V^{as} is the asymptotic fraction of the immunized in the population

$$V^{\text{as}} = (1 - d) \frac{a}{1 + \omega/v_r}.$$

183 The resulting values differ depending on the setups of vaccine effectiveness a , revaccination
184 rate v_r , the fraction of never-vaccinated population d and immunity waning rate ω (Tab. 1).
185 Even for the most optimistic setup (high $a = 0.9$, high $v_r = 0.008$, low $d = 0.1$, low $\omega =$
186 0.002) we obtain $V^{\text{as}} = 0.65$, and $f_{\min} = 0.29$. Compared to the current strict restrictions
187 required to contain COVID-19 in some countries, the level of 0.29 restrictions is lower, but it is
188 a considerable reduction of freedom compared to before the pandemic. All remaining realistic
189 parameter setups require high f_{\min} , ranging between 0.46 (for the reference setup) and 0.68 (for
190 the increased d , increased ω as compared to the reference).

191 **Discussion**

192 Introducing VPs is widely seen as a means to opening up economies and societies, despite the
193 ongoing epidemic. To inform this discussion, we extend a SIR model to reflect vaccination
194 dynamics and possibly different restrictions for VP holders. A wide range of model parameter
195 choices show the possibility of an epidemic resurgence, even for optimistic parameter setups.
196 The main driver of this phenomenon is the potential lack of immunity of VP holders. With a
197 VP, people enjoy low restrictions while actually being susceptible and potentially contagious
198 because the vaccine was ineffective or the immunity has waned.

199 VAP-SIRS deliberately keeps several aspects simple (see Methods for model limitations).

	Parameter setup	a	v_r	d	ω	V^{as}	f_{min}
1	Reference setup (ref Fig. 3a)	0.9	0.004	0.1	0.002	0.54	0.46
2	Decreased a (ref Fig. 3b)	0.6	0.004	0.1	0.002	0.36	0.61
3	Increased v_r (ref Fig. 3c)	0.9	0.008	0.1	0.002	0.65	0.29
4	Increased d (ref Fig. 3e)	0.9	0.004	0.3	0.002	0.42	0.57
5	Increased ω (ref Fig. 3f)	0.9	0.004	0.1	0.005	0.36	0.61
6	Decreased a and increased v_r	0.6	0.008	0.1	0.002	0.43	0.56
7	Decreased a and increased d	0.6	0.004	0.3	0.002	0.28	0.65
8	Decreased a and increased ω	0.6	0.004	0.1	0.005	0.24	0.67
9	Increased v_r , increased d	0.9	0.008	0.3	0.002	0.50	0.50
10	Increased v_r , increased ω	0.9	0.008	0.1	0.005	0.50	0.50
11	Increased d , increased ω	0.9	0.004	0.3	0.005	0.21	0.68

Table 1: **Asymptotic level of immunization V^{as} and minimum common restrictions f_{min} for different parameter setups**, for parameters: vaccine effectiveness a , revaccination rate v_r , fraction of never-vaccinated d , and waning immunity rate ω . The first row concerns the reference setup; rows below are setups with the same parameters as in the reference setup, but with either one parameter changed (in bold; rows 2–5; same as in Figure 3, apart from preferential mixing, as it is not relevant for common restrictions) or two parameters changed (in bold; rows 6–11).

200 The advantage of our analysis is the relevance for long-term dynamics, and the focus on avoid-
 201 ing epidemic resurgence. Avoiding another wave is a prudent goal due to threats it poses, in the
 202 form of long-term health effects, the deleterious impact on societies and the emergence of new
 203 variants.

204 Our model gives valuable insights into policies pertaining to the introduction of VPs. Model
 205 analyses suggest that considerably lowering restrictions for VP holders is only possible when
 206 keeping high restrictions on the rest of the population. This situation seems tolerable for the un-
 207 vaccinated only given high vaccine availability and vaccination speed. The alternative cautious
 208 option, i.e. not granting freedoms for VP holders, defeats the purpose of the instrument. Once
 209 a large part of the population has been vaccinated, policymakers need to find a new, common
 210 restriction level, which could also be achieved through temporary VPs. Our model implies that
 211 such common restrictions need to be higher than those initially granted to VP holders, and need
 212 to be introduced in time to avoid another wave.

213 As expected, the model shows that there is a larger selection of admissible restrictions’
 214 setups under high vaccine effectiveness, slowly waning immunity, proportional social mixing,
 215 low share of never-vaccinated and higher vaccination rate. At least the latter two parameters
 216 are amenable to policy action. Thus, efforts to increase (re-) vaccination speed and encour-

217 age people to get vaccinated also extend the margin of lowering restrictions for VP holders as
218 well as eventual common restrictions. Social mixing patterns, such as preferential mixing, can
219 accelerate the infection resurgence in time and, although difficult to change by policymaking,
220 should be monitored. Finally, it is noteworthy that VP holders are less likely to be tested, as they
221 are assumed to be protected and they may exhibit milder symptoms. Therefore, their potential
222 infection is more likely to remain undetected, resulting in an effect similar to that of lowering
223 restrictions. To prevent undesirable outcomes, the testing criteria should not exclude the VP
224 holders. In addition, the VP holders should be widely and regularly tested for antibody level,
225 aiming at detection of such vaccinated that have lost, or have never gained, immunity. Finally,
226 temporary VPs could be considered, with their prolongation conditioned on high antibody level
227 or recent (re-)vaccination.

228 **References**

- 229 1. *International health regulations (2005)* Third edition (ed World Health Organization)
230 (World Health Organization, Geneva, Switzerland, 2016).
- 231 2. Voo, T. C. *et al.* Immunity certification for COVID-19: ethical considerations. *Bulletin of*
232 *the World Health Organization* **99**, 155–161 (2021).
- 233 3. Brown, R. C. H., Kelly, D., Wilkinson, D. & Savulescu, J. The scientific and ethical feasi-
234 bility of immunity passports. *The Lancet Infectious Diseases* **21**, e58–e63 (2021).
- 235 4. European Commission, Directorate-General for Justice and Consumers. *Proposal for a*
236 *REGULATION OF THE EUROPEAN PARLIAMENT AND OF THE COUNCIL on a*
237 *framework for the issuance, verification and acceptance of interoperable certificates on*
238 *vaccination, testing and recovery to facilitate free movement during the COVID-19 pan-*
239 *demic (Digital Green Certificate, Document 52021PC0130)* <https://eur-lex.europa.eu/legal-content/EN/TXT/?uri=CELEX:52021PC0130> (2021).
- 240
241 5. World Health Organization. *"Immunity passports" in the context of COVID-19* tech. rep.
242 (WHO). <https://www.who.int/news-room/commentaries/detail/immunity-passports-in-the-context-of-covid-19> (2021).
- 243

- 244 6. Voysey, M. *et al.* Single-dose administration and the influence of the timing of the booster
245 dose on immunogenicity and efficacy of ChAdOx1 nCoV-19 (AZD1222) vaccine: a pooled
246 analysis of four randomised trials. *The Lancet* **397**, 881–891 (2021).
- 247 7. Thompson, M. G. *et al.* Interim Estimates of Vaccine Effectiveness of BNT162b2 and
248 mRNA-1273 COVID-19 Vaccines in Preventing SARS-CoV-2 Infection Among Health
249 Care Personnel, First Responders, and Other Essential and Frontline Workers — Eight
250 U.S. Locations, December 2020–March 2021. *MMWR. Morbidity and Mortality Weekly
251 Report* **70**, 495–500 (2021).
- 252 8. Bian, L. *et al.* Effects of SARS-CoV-2 variants on vaccine efficacy and response strategies.
253 *Expert Review of Vaccines*, 1–9 (2021).
- 254 9. Chia, W. N. *et al.* Dynamics of SARS-CoV-2 neutralising antibody responses and duration
255 of immunity: a longitudinal study. *The Lancet Microbe*. [https://doi.org/10.](https://doi.org/10.1016/s2666-5247(21)00025-2)
256 [1016/s2666-5247\(21\)00025-2](https://doi.org/10.1016/s2666-5247(21)00025-2) (2021).
- 257 10. Iyer, A. S. *et al.* Persistence and decay of human antibody responses to the receptor bind-
258 ing domain of SARS-CoV-2 spike protein in COVID-19 patients. *Science Immunology* **5**,
259 eabe0367 (2020).
- 260 11. Hall, V. J. *et al.* SARS-CoV-2 infection rates of antibody-positive compared with antibody-
261 negative health-care workers in England: a large, multicentre, prospective cohort study
262 (SIREN). *The Lancet* **397**, 1459–1469 (2021).
- 263 12. Hansen, C. H., Michlmayr, D., Gubbels, S. M., Mølbak, K. & Ethelberg, S. Assessment of
264 protection against reinfection with SARS-CoV-2 among 4 million PCR-tested individuals
265 in Denmark in 2020: a population-level observational study. *The Lancet* **397**, 1204–1212
266 (2021).
- 267 13. Sadarangani, M. *et al.* Importance of COVID-19 vaccine efficacy in older age groups.
268 *Vaccine* **39**, 2020–2023 (2021).
- 269 14. Prieto Curiel, R. & González Ramírez, H. Vaccination strategies against COVID-19 and
270 the diffusion of anti-vaccination views. *Scientific Reports* **11**, 6626 (2021).

- 271 15. Moore, S., Hill, E. M., Tildesley, M. J., Dyson, L. & Keeling, M. J. Vaccination and non-
272 pharmaceutical interventions for COVID-19: a mathematical modelling study. *The Lancet*
273 *Infectious Diseases* (2021).
- 274 16. Lee, B. Y. *et al.* Vaccination Deep Into a Pandemic Wave. *American Journal of Preventive*
275 *Medicine* **39**, e21–e29 (2010).
- 276 17. Jentsch, P. C., Anand, M. & Bauch, C. T. Prioritising COVID-19 vaccination in chang-
277 ing social and epidemiological landscapes: a mathematical modelling study. *The Lancet*
278 *Infectious Diseases* (2021).
- 279 18. Bubar, K. M. *et al.* Model-informed COVID-19 vaccine prioritization strategies by age
280 and serostatus. *Science* **371**, 916–921 (2021).
- 281 19. Bauer, S. *et al.* Relaxing restrictions at the pace of vaccination increases freedom and
282 guards against further COVID-19 waves in Europe. *arXiv:2103.06228 [q-bio]*. arXiv:
283 2103.06228. <http://arxiv.org/abs/2103.06228> (2021).
- 284 20. Giordano, G. *et al.* Modeling vaccination rollouts, SARS-CoV-2 variants and the require-
285 ment for non-pharmaceutical interventions in Italy. *Nature Medicine* (2021).
- 286 21. Moghadas, S. M. *et al.* Evaluation of COVID-19 vaccination strategies with a delayed
287 second dose. *PLOS Biology* **19** (ed Read, A. F.) e3001211 (2021).
- 288 22. Makhoul, M. *et al.* Epidemiological Impact of SARS-CoV-2 Vaccination: Mathematical
289 Modeling Analyses. *Vaccines* **8**, 668 (2020).
- 290 23. Keeling, M. J. & Rohani, P. *Modeling Infectious Diseases in Humans and Animals* (2021)
291 (Princeton University Press, Sept. 2011).
- 292 24. Ritchie, H. *et al.* *Coronavirus (COVID-19) Vaccinations* [https://ourworldindata.](https://ourworldindata.org/covid-vaccinations)
293 [org/covid-vaccinations](https://ourworldindata.org/covid-vaccinations) (2021).
- 294 25. European Centre for Disease Prevention and Control (ECDC). *COVID-19 Vaccine Tracker*
295 [https://vaccinetracker.ecdc.europa.eu/public/extensions/](https://vaccinetracker.ecdc.europa.eu/public/extensions/COVID-19/vaccine-tracker.html)
296 [COVID-19/vaccine-tracker.html](https://vaccinetracker.ecdc.europa.eu/public/extensions/COVID-19/vaccine-tracker.html) (2021).

- 297 26. Hung, I. F. N. & Poland, G. A. Single-dose Oxford–AstraZeneca COVID-19 vaccine fol-
298 lowed by a 12-week booster. *The Lancet* **397**, 854–855 (2021).
- 299 27. Emary, K. R. W. *et al.* Efficacy of ChAdOx1 nCoV-19 (AZD1222) vaccine against SARS-
300 CoV-2 variant of concern 202012/01 (B.1.1.7): an exploratory analysis of a randomised
301 controlled trial. *The Lancet* **397**, 1351–1362 (2021).
- 302 28. Polack, F. P. *et al.* Safety and Efficacy of the BNT162b2 mRNA Covid-19 Vaccine. *New*
303 *England Journal of Medicine* **383**, 2603–2615 (2020).
- 304 29. Dagan, N. *et al.* BNT162b2 mRNA Covid-19 Vaccine in a Nationwide Mass Vaccination
305 Setting. *New England Journal of Medicine* **384**, 1412–1423 (2021).
- 306 30. Letizia, A. G. *et al.* SARS-CoV-2 seropositivity and subsequent infection risk in healthy
307 young adults: a prospective cohort study. *The Lancet Respiratory Medicine* (2021).
- 308 31. Rockstroh, A. *et al.* Correlation of humoral immune responses to different SARS-CoV-2
309 antigens with virus neutralizing antibodies and symptomatic severity in a German COVID-
310 19 cohort. *Emerging Microbes & Infections* **10**, 774–781 (2021).
- 311 32. Wajnberg, A. *et al.* Robust neutralizing antibodies to SARS-CoV-2 infection persist for
312 months. *Science* **370**, 1227–1230 (2020).
- 313 33. The COVID-19 Genomics UK (COG-UK) consortium *et al.* Assessing transmissibility of
314 SARS-CoV-2 lineage B.1.1.7 in England. *Nature* (2021).
- 315 34. Davies, N. G. *et al.* Estimated transmissibility and impact of SARS-CoV-2 lineage B.1.1.7
316 in England. *Science* **372**, eabg3055 (2021).

1 **Methods**

2 **Mathematical model**

3 We introduce a modified susceptible-infectious-recovered-susceptible (SIRS) model [1] (Figure
4 1a). The population is divided into two subpopulations: those who are not vaccinated (S, I, R)
5 and those who got vaccinated at least once (S_V, I_V, R_V, V). We assume that the group of
6 non-vaccinated susceptible individuals S (and, similarly, infected I and recovered R) is divided
7 into two subgroups: S_N and S_D . The S_N compartment contains such susceptible who will
8 eventually be vaccinated, while those in S_D will not. The S_D compartment contains not only
9 the subpopulation of children, who are currently not included in the vaccination program, but
10 also those who for health reasons cannot be vaccinated, and finally, individuals who do not
11 vaccinate because of hesitancy.

12 The S_N population is vaccinated with rate v and effectiveness a . Consequently, the individuals
13 from the S_N group populate the vaccinated group V with rate av . The individuals in V are
14 considered immune, and we assume that immunization prevents them both from getting infected
15 and infecting others. The S_V compartment is composed of S_1 and S_2 (and, similarly, vaccinated
16 infected I_V consists of I_1 and I_2). Due to vaccine ineffectiveness, people in S_1 are perceived
17 as immunized, but in fact are susceptible. S_1 is populated from S_N with rate $(1 - a)v$. The
18 vaccinated from the V group move to the S_2 group of susceptibles with immunity waning rate
19 ω . The individuals from the S_1 group move to S_2 with the same rate ω . The S_2 group is the
20 group of vaccinated, but no longer immune, and thus, susceptible individuals. In contrast to
21 S_1 , we consider that the S_2 group is subject to revaccination. Consequently, a fraction of size
22 a of the population from S_2 populates V with rate av_r and a fraction of size $(1 - a)$ populates
23 S_1 with rate $(1 - a)v_r$. Across the manuscript, we assume $v_r = v$, but the model is general
24 and different values can be considered. Individuals from S_1 move to S_2 with rate ω to ensure
25 that the ineffectively vaccinated are revaccinated with the same speed as the ones for which the
26 vaccine was effective.

27 Some of the susceptibles in S_1 (or, similarly, S_2) may not get revaccinated fast enough and
28 may become infected and populate I_1 (or, I_2). Then, as in the classical SIRS model, the I_1 (or

29 I_2) population recovers and populates group R_V with rate γ . We consider that the recovered in
30 R_V may also lose the immunity, and become susceptible again and move to S_2 with rate κ . We
31 fix κ to 0.002, corresponding to average 500 days duration of natural immunity. There remains
32 uncertainty regarding the waning time for natural immunity, but early evidence indicates it lasts
33 at least 180 days [2, 3, 4]. Hence, we assume an optimistic scenario of natural immunity lasting
34 similarly long as the immunity gained via vaccination. Before the recovered in the R_V lose
35 immunity, they might be revaccinated, and, thus, populate the V group with rate v_r .

36 The remaining susceptible subgroups (the S_N and S_D) may undergo the same classical
37 dynamics, i.e., become infected, recover, and either become susceptible again or, in case of
38 the recovered in the R_N subgroup, become vaccinated with rate v .

39 Note that for the recovered in the R_V or R_N groups we assume that vaccination effectiveness
40 is 1, which is substantiated on the basis of the fact that vaccination combined with a previous
41 infection should confer a much stronger protection than only vaccination of a susceptible individual.

42 The following parameters are used to describe population dynamics in the model:

- f_v, f : restrictions level (for VP holders and others)
- β_0 : basic transmission rate
- β_v, β : transmission rate (for VP holders and others)
- γ : recovery rate
- κ : natural immunity waning rate
- a : vaccination effectiveness
- v : vaccination rate
- v_r : revaccination rate
- ω : vaccine-induced immunity waning rate
- d : fraction of population that will never get vaccinated

43 Finally, the following set of ordinary differential equations (ODEs) defines the dynamics

$$\begin{aligned}
 \frac{d}{dt}S_D &= -(\beta I + \beta I_V)S_D + \kappa R_D, \\
 \frac{d}{dt}S_N &= -(\beta I + \beta I_V)S_N - vS_N + \kappa R_N, \\
 \frac{d}{dt}S_1 &= v_r(1-a)S_2 + v(1-a)S_N - \omega S_1 - (\beta I + \beta_v I_V)S_1, \\
 \frac{d}{dt}S_2 &= -v_r S_2 + \omega V + \omega S_1 - (\beta I + \beta_v I_V)S_2 + \kappa R_V, \\
 \frac{d}{dt}V &= vaS_N + v_r a S_2 - \omega V + v_r R_V + vR_N, \\
 \frac{d}{dt}I_D &= (\beta I + \beta I_V)S_D - \gamma I_D, \\
 \frac{d}{dt}I_N &= (\beta I + \beta I_V)S_N - \gamma I_N, \\
 \frac{d}{dt}I_1 &= (\beta I + \beta_v I_V)S_1 - \gamma I_1, \\
 \frac{d}{dt}I_2 &= (\beta I + \beta_v I_V)S_2 - \gamma I_2, \\
 \frac{d}{dt}R_V &= \gamma I_V - \kappa R_V - v_r R_V, \\
 \frac{d}{dt}R_D &= \gamma I_D - \kappa R_D, \\
 \frac{d}{dt}R_N &= \gamma I_N - \kappa R_N - vR_N,
 \end{aligned} \tag{1}$$

44 where also the following relations hold

$$\begin{aligned}
 S_V &= S_1 + S_2, \\
 I_V &= I_1 + I_2, \\
 S &= S_D + S_N, \\
 I &= I_D + I_N, \\
 R &= R_N + R_D,
 \end{aligned}$$

45 with the constraint $S, S_V, I, I_V, R, R_V \geq 0$. Finally, to consider the subpopulation dynamics in
 46 terms of fractions of the entire subpopulation, we set

$$S + S_V + I + I_V + R + R_V = 1 \tag{2}$$

and denote d to be the fraction of the never-vaccinated population

$$d = S_D + I_D + R_D.$$

47 **Modeling restrictions**

48 We assume that the VP holders consist of the following subpopulations of vaccinated at least
49 once: V, S_V, I_V, R_V . Recall that the net effect of all non-pharmaceutical interventions is modeled
50 using parameters f_v and f , called restrictions throughout the text. The parameter f_v amounts to
51 the level of restriction of contacts, and thus the ability to infect, within the group of VP holders.
52 The parameter f satisfies $f \geq f_v$ and corresponds to restriction of contacts within the rest of
53 the population, as well as between the VP holders and the rest of the population.

54 The restriction level f_v for the VP holders is introduced in the model as a modulator of the
55 transmission rate β_v . Specifically, we assume that $\beta_v = \beta_0(1 - f_v)$, where β_0 is the transmission
56 rate of the SARS-CoV-2 virus without restrictions. We assume f_v ranges from 0 to 1, where
57 $f_v = 0$ corresponds to no restrictions enforced on the VP holders, and $f_v = 1$ corresponding to
58 full restrictions. Given that for $f_v = 0$ the reproduction number $R_{\max} = \beta_0/\gamma = 4$, and that the
59 recovery rate $\gamma = 1/6$, we obtain the no-restriction transmission rate $\beta_0 = 2/3$.

60 Similarly, the transmission rate parameter $\beta = \beta_0(1 - f)$ describes the transmission rate
61 within the rest of the population and between VP holders and the rest, given the restrictions f .

62 **Proportional versus preferential types of social mixing**

63 The above described model equations are based on the assumption that the social mixing
64 between social groups in the population is proportional to the group sizes (the mass action
65 principle). Instead, preferential mixing can be assumed, where the VP holders are more likely
66 to contact other VP holders, since they have lower restrictions [5]. This preferential bias is
67 proportional to the difference between the restrictions f and f_v . To incorporate the preferential
68 mixing effect in the ODE model (Equation 1) we rescale the interaction terms according to the

69 following rules:

$$S_V I_V \rightarrow \frac{\beta_v}{\beta(S + I + R) + \beta_v(1 - (S + I + R))} S_V I_V$$

$$S I_V \rightarrow \frac{\beta}{\beta(S + I + R) + \beta_v(1 - (S + I + R))} S I_V$$

70 where $S + I + R$ is the non-immune population.

71 Model simulations

72 For simulations, we solve the model numerically by means of joint Adams' and BDF methods,
 73 as implemented in the R package deSolve, lsoda method of the ode function [6]. The method
 74 monitors data in order to select between non-stiff (Adams') and stiff (BDF) methods. It uses
 75 the non-stiff method initially [7].

76 To generate the data presented in Figure 1b,c, we use the reference setup of parameters:
 77 $\beta_0 = 2/3$, $f = 0.63$ (and thus $\beta = 0.247$), $f_v = 0.05$ (and thus $\beta_v = 0.634$), $\gamma = 1/6$,
 78 $\kappa = 1/500$, $a = 0.9$, $v = v_r = 1/250$, $\omega = 1/500$, $d = 0.1$, with initial conditions $I = 10^{-6}$,
 79 $I_D = d \cdot I = 10^{-7}$; $I_N = (1 - d) \cdot I = 0.9 \cdot 10^{-6}$, $R = 0$, $V = 0$. Given $I(t)$ resulting
 80 from the solution of the model's ODE system, to present the final results as easier interpretable
 81 cases per milion rather than fractions, we re-scale the results by 1M. Additionally, we compute
 82 a proxy for the daily incidence number of new cases from the following relation between $I(t)$
 83 and $I^*(t)$:

$$I(t) = \int_0^t e^{-\gamma(t-\tau)} I^*(\tau) d\tau$$

$$= \int_{t-1}^t e^{-\gamma(t-\tau)} I^*(\tau) d\tau + e^{-\gamma} \int_0^{t-1} e^{-\gamma(t-1-\tau)} I^*(\tau) d\tau$$

$$\simeq \frac{1}{\gamma} I^*(t) (1 - e^{-\gamma}) + e^{-\gamma} I(t-1).$$

84 Thus, the $I^*(t)$ is computed as

$$I^*(t) \simeq \frac{\gamma}{1 - e^{-\gamma}} (I(t) - e^{-\gamma} I(t-1)).$$

85 We proceed similarly to obtain daily incidence numbers I_1^* , I_2^* and for the sum of all infected,
 86 and again to make it interpretable in the figures we re-scale it by 1M.

87 **Stability analysis**

88 The vaccination dynamics can be solved explicitly in the absence of infections. Fixing $I =$
 89 $I_V = R = R_V = 0$, and assuming $v = v_r$, we obtain

$$\begin{aligned} S(t) &= d + (1 - d)e^{-vt}, \\ V(t) &= (1 - d) \frac{va}{va + \omega} (1 - e^{-(va+\omega)t}), \\ S_V(t) &= 1 - S - V. \end{aligned}$$

90 For convenience, where it is not needed, we drop the time argument.

Taking an adiabatic approach we linearize the infection dynamics for small I , I_V and R under the assumption of slowly varying S , S_V and V . In that case, the infection dynamics decouples from the vaccination dynamics and the Jacobian submatrix J_{sub} for the equations for I and I_V is given by:

$$J_{sub} = \begin{pmatrix} \beta S - \gamma & \beta S \\ \beta S_V & \beta_V S_V - \gamma \end{pmatrix}.$$

91 Given the Jacobian submatrix, we can approximate the dynamics in a small neighborhood of
 92 the $I = I_V = 0$ state as

$$\begin{pmatrix} \frac{d}{dt} I \\ \frac{d}{dt} I_V \end{pmatrix} = \begin{pmatrix} \beta S - \gamma & \beta S \\ \beta S_V & \beta_V S_V - \gamma \end{pmatrix} \cdot \begin{pmatrix} I \\ I_V \end{pmatrix}. \quad (3)$$

93 **The instantaneous reproduction number R^* and the instantaneous doubling time D**

94 Since the largest and the second largest eigenvalues λ_{\max} and λ_2 of J_{sub} are both real, the
 95 solution to Equation 3 providing the dynamics of infection numbers of the vaccinated and the

96 rest of the population in time can be written in the following form

$$\begin{pmatrix} I(t) \\ I_V(t) \end{pmatrix} = c_1 w_1 e^{\lambda_{\max} t} + c_2 w_2 e^{\lambda_2 t} = e^{\lambda_{\max} t} (c_1 w_1 + c_2 w_2 e^{(\lambda_2 - \lambda_{\max}) t}), \quad (4)$$

97 where w_1 and w_2 are the respective eigenvectors, and c_1 and c_2 are constants depending on the
98 initial conditions.

99 Since we have $\lambda_2 - \lambda_{\max} \leq 0$, we can approximate the time evolution of infection numbers
100 by

$$\begin{pmatrix} I(t) \\ I_V(t) \end{pmatrix} \approx c_1 w_1 e^{\lambda_{\max} t}. \quad (5)$$

101 The largest eigenvalue of J_{sub} is given by

$$\lambda_{\max} = \frac{1}{2} S \beta - \gamma + \frac{1}{2} S_V \beta_v + \frac{1}{2} \sqrt{S^2 \beta^2 + S_V^2 \beta_v^2 - 2 S S_V \beta \beta_v + 4 S S_V \beta^2}, \quad (6)$$

102 whereby it is convenient to express λ_{\max} as a function of $R_1 = \frac{\beta}{\gamma}$ and $R_2 = \frac{\beta_v}{\gamma}$. We then obtain

$$\lambda_{\max} = \gamma \left(\frac{1}{2} (R_1 S + R_2 S_V) + \frac{1}{2} \sqrt{(R_1 S - R_2 S_V)^2 + 4 S S_V R_1^2} - 1 \right). \quad (7)$$

103 Given the population fractions $S(t)$ and $S_V(t)$ at a given time instant t , the linearized
104 dynamics of infections given by Equation 3 has a corresponding two-type Galton-Watson branching
105 process, which is a microscopic description of the dynamics. The two types of the process
106 correspond to the I and I_V groups. The type I individuals generate $Pois(R_1 S)$ offsprings of
107 type I and $Pois(R_1 S_V)$ offsprings of type I_V . The type I_V individuals generate $Pois(R_1 S)$
108 offsprings of type I and $Pois(R_2 S_V)$ offsprings of type I_V . The linearized dynamics (3) can
109 then be understood as a mean field limit of the microdynamics described by such a branching
110 process. Moreover, the spectral norm

$$R^* = \frac{1}{2} (R_1 S + R_2 S_V) + \frac{1}{2} \sqrt{4 R_1^2 S S_V + (R_1 S - R_2 S_V)^2} \quad (8)$$

of the transition matrix

$$\begin{pmatrix} R_1 S & R_1 S_V \\ R_1 S & R_2 S_V \end{pmatrix}$$

111 of the branching process can be interpreted as the reproduction number of the branching process,
 112 since the expected number of infected in generation n grows like $const \cdot (R^*)^n$ [8]. We refer to
 113 R^* as the instantaneous reproduction number. The term instantaneous comes from the fact that
 114 we are considering the linearized adiabatic dynamics in a small neighborhood of the $I = I_V = 0$
 115 (ref Eq. 3).

The above discrete branching process can be extended to a continuous time branching process by assuming a probability distribution on the generation time, denoted $\varphi(\gamma)$. The growth of the continuous time branching process $const \cdot e^{\alpha t}$ is characterized by its Malthusian growth parameter, denoted α . The relation between the instantaneous reproduction number R^* , the distribution $\varphi(\tau)$ and the Malthusian parameter α for such a branching process is given by

$$R^* \cdot \mathcal{L}_\varphi(\alpha) = 1$$

116 where $\mathcal{L}_\varphi(\alpha)$ is the Laplace transform $\int_0^\infty e^{-\alpha\tau} \varphi(\tau) d\tau$ of the distribution φ [8]. Since the setting
 117 of ODE model (1) implies exponential distribution of the generation time, i.e, $\varphi(\gamma) = Exp(\gamma)$,
 118 the following relation holds: $\alpha = \gamma(R^* - 1)$.

119 By Equation 5, the Malthusian parameter α for our dynamics is given by the largest eigenvalue
 120 λ_{\max} . Hence we obtain the relation between the instantaneous reproduction R^* and the λ_{\max} as
 121 $\lambda_{\max} = \gamma(R^* - 1)$. Note that since both S and S_V are functions of time, so are λ_{\max} and R^* .

122 It is noteworthy that in the above equations, all R_1 , R_2 , $R_1 S$ and $R_2 S_V$, and R^* should be
 123 seen as reproduction numbers, but of a different nature [9]. R_1 and R_2 are reproduction numbers
 124 taking into account the restrictions f and f_v , respectively. The $R_1 S$ and $R_2 S_V$ are also group
 125 specific, but in addition incorporate the respective group sizes. Finally, R^* combines all these
 126 factors together.

127 Having this and Equation 5, we define the instantaneous doubling time at time, denoted t
 128 $D(t)$, as the solution D of $e^{\gamma(R^*(t)-1) \cdot D} = 2$. Such obtained doubling times are featured in
 129 Figure 2b.

130 **The times of transitions between subcritical and overcritical epidemics**

The analysis of the linearized dynamics around $I = I_V = 0$ allows us to determine transitions between subcritical and overcritical epidemics. Such transitions occur at the time instants t at which $\lambda_{\max}(t) = 0$, or, equivalently, at $R^*(t) = 1$. We thus find that for given values of $S(t)$ and $S_V(t)$ the critical times t for transitions between subcritical and overcritical epidemics are the roots of the equation

$$\lambda_{\max}(t) = 0.$$

131 The obtained critical threshold times are plotted in the lower triangles of the panels in Figure 3
132 in the main text. In the case of proportional mixing the above equation is equivalent to:

$$(R_1 S(t) - 1) (R_2 S_V(t) - 1) = R_1^2 S(t) S_V(t).$$

133 **Asymptotic structure of the population**

134 The asymptotic structure of the population in terms of the sizes of the subpopulations V , S_V
135 and S_D can be easily obtained by setting $I = I_V = R = R_V = 0$ and computing the stable
136 stationary solution for V^{as} , S^{as} and S_V^{as} of our ODE system (1):

$$\begin{aligned} S^{\text{as}} &= d \\ S_V^{\text{as}} &= (1 - d)(1 - \eta) \\ V^{\text{as}} &= (1 - d)\eta \\ S^{\text{as}} + S_V^{\text{as}} &= 1 - V^{\text{as}}, \end{aligned}$$

where

$$\eta = \frac{a}{1 + \omega/v_r}$$

137 can be seen as the actual immunization rate in the population, and is expressed as a function
138 of vaccine effectiveness a and the ratio of the immunity waning rate ω and the revaccination
139 rate v_r . The obtained values correspond to the structure in the limit $t \rightarrow \infty$ and represent the
140 structure to which the population converges in the long term.

141 Having this, we obtain the asymptotic instantaneous reproduction number R^* by inserting
142 the asymptotic values S^{as} and S_V^{as} into Equation 8. These values are plotted in the upper
143 triangles in the panels of Figure 3 in the main text.

Finally, we solve for such minimum common restrictions $f = f_v = f_{\text{min}}$, which will result in instantaneous reproduction number $R^* = 1$ for the different vaccine effectiveness and vaccination rate setups. Hence f_{min} is found from $R_{\text{max}}(1 - f_{\text{min}}) = 4(1 - f_{\text{min}}) = \frac{1}{1-V}$ as

$$f_{\text{min}} = \max\left(0, 1 - \frac{1}{4(1 - V^{\text{as}})}\right).$$

144 **Model limitations**

145 VAP-SIRS is not compartmentalized for age groups and does not consider deaths or healthcare
146 system limitations like some other models, albeit in the context of exploring different parameters
147 than larger freedom for VP holders [10, 11, 12, 13, 14, 15]. Deaths could be taken into
148 account through a straightforward modification of the model, which would however lead to
149 more parameters. In this case, the fact that vaccination reduces the risk of death would have to
150 be accounted for. The impact of deaths on public health and society, which is very important
151 especially when the epidemic becomes overcritical, can be indirectly assessed based on the
152 number of infection cases. In general, features such as age groups and deaths, however, do not
153 add further insights into the questions which are the focus of our study, namely, the long-term
154 effects of VPs and avoiding overcritical dynamics. In this context, the advantage of our model is
155 that it is enriched in features such as revaccinations and waning immunity, which are particularly
156 relevant in the long term.

157 Nevertheless, possible extensions to our model could include inter- individual or age-dependent
158 variations in immunity, which is also relevant for people with severe chronic conditions or
159 immunodeficiencies, or changes in behaviour over time. The presented analysis has been
160 performed assuming that without restrictions, the maximum reproduction number of the virus
161 is $R_{\text{max}} = 4$. More transmittable variants could easily be modeled by fixing higher values of
162 R_{max} . Similarly, our results do not account for the possibility of immune escape variants, but
163 such variants could be considered using our model by fixing smaller vaccine effectiveness than

164 the values we considered. Asymptotic endemic states of the ODE system (1) could easily be
165 computed, but are not discussed here due to space constraints. Finally, another limitation of
166 our analysis is that not all parameter values are exactly known, such as the post- vaccination
167 or natural immunity waning time. We, however, fix optimistic values for such parameters, and
168 show that unfavorable infection dynamics can still be obtained even under optimistic assumptions.

169 **Data Availability**

170 Not applicable

171 **Code Availability**

172 The VAP-SIRS model was implemented using R version 4.0.2 along with the shiny package
173 to build an interactive web application that allows to simulate the model. The code of the
174 model is available online in the GitHub repository: [https://github.com/storaged/
175 VAP-SIRS](https://github.com/storaged/VAP-SIRS), and the on-line tool is available [http://bioputer.mimuw.edu.pl:85/
176 VAP-SIRS/](http://bioputer.mimuw.edu.pl:85/VAP-SIRS/). The code to generate Fig 2 and Fig 3 from the main text is available at [https:
177 //github.com/eMaerthin/Fig2_Fig3](https://github.com/eMaerthin/Fig2_Fig3).

178 **References**

- 179 1. Keeling, M. J. & Rohani, P. *Modeling Infectious Diseases in Humans and Animals* (Princeton
180 University Press, 2011).
- 181 2. Tarke, A. *et al.* Negligible impact of SARS-CoV-2 variants on CD4+ and CD8+ T cell
182 reactivity in COVID-19 exposed donors and vaccinees. *bioRxiv*. [https://www.biorxiv.
183 org/content/early/2021/03/01/2021.02.27.433180](https://www.biorxiv.org/content/early/2021/03/01/2021.02.27.433180) (2021).
- 184 3. Chia, W. N. *et al.* Dynamics of SARS-CoV-2 neutralising antibody responses and duration
185 of immunity: a longitudinal study. *The Lancet Microbe* (2021).
- 186 4. Zuo, J. *et al.* Robust SARS-CoV-2-specific T cell immunity is maintained at 6 months
187 following primary infection. *Nature Immunology* (2021).

- 188 5. Marschner, I. C. The effect of preferential mixing on the growth of an epidemic. *Mathematical*
189 *Biosciences* **109**, 39–67 (1992).
- 190 6. Soetaert, K., Petzoldt, T. & Setzer, R. W. Solving Differential Equations in R: PackagedeSolve.
191 *Journal of Statistical Software* **33** (2010).
- 192 7. Hindmarsh, A. C. & Petzold, L. R. Algorithms and software for ordinary differential
193 equations and differential- algebraic equations, Part II: Higher-order methods and software
194 packages. *Computers in Physics* **9**, 148 (1995).
- 195 8. Athreya, K. B. & Ney, P. E. *Branching Processes* German. OCLC: 863789203 (1972).
- 196 9. Van den Driessche, P. Reproduction numbers of infectious disease models. *Infectious*
197 *Disease Modelling* **2**, 288–303 (2017).
- 198 10. Sadarangani, M. *et al.* Importance of COVID-19 vaccine efficacy in older age groups.
199 *Vaccine* **39**, 2020–2023 (2021).
- 200 11. Moore, S., Hill, E. M., Tildesley, M. J., Dyson, L. & Keeling, M. J. Vaccination and
201 non-pharmaceutical interventions for COVID-19: a mathematical modelling study. *The*
202 *Lancet Infectious Diseases* (2021).
- 203 12. Jentsch, P. C., Anand, M. & Bauch, C. T. Prioritising COVID-19 vaccination in changing
204 social and epidemiological landscapes: a mathematical modelling study. *The Lancet Infectious*
205 *Diseases* (2021).
- 206 13. Bubar, K. M. *et al.* Model-informed COVID-19 vaccine prioritization strategies by age
207 and serostatus. *Science* **371**, 916–921 (2021).
- 208 14. Bauer, S. *et al.* Relaxing restrictions at the pace of vaccination increases freedom and
209 guards against further COVID-19 waves in Europe. *arXiv:2103.06228 [q-bio]*. arXiv:
210 2103.06228. <http://arxiv.org/abs/2103.06228> (2021).
- 211 15. Giordano, G. *et al.* Modeling vaccination rollouts, SARS-CoV-2 variants and the requirement
212 for non-pharmaceutical interventions in Italy. *Nature Medicine* (2021).

213 **End notes**

214 **Acknowledgements**

215 SC acknowledges support by University of Malta. TC has received funding from the European
216 Union's Horizon 2020 research and innovation programme under grant agreement No 101016233
217 (PERISCOPE) GG acknowledges support by the University of Trento within the COVID-19
218 Strategic Project MOSES (Models for Reasoning about the Spreading of Diseases). MP was
219 supported by the Slovenian Research Agency (Grant Nos. P1-0403 and J1-2457). EP acknowledges
220 support by the University of Crete. ES acknowledges funding by the Polish National Science
221 Centre OPUS grant no 2019/33/B/NZ2/00956 and SONATA-BIS grant no 2020/38/E/NZ2/00305.

222 **Author contributions**

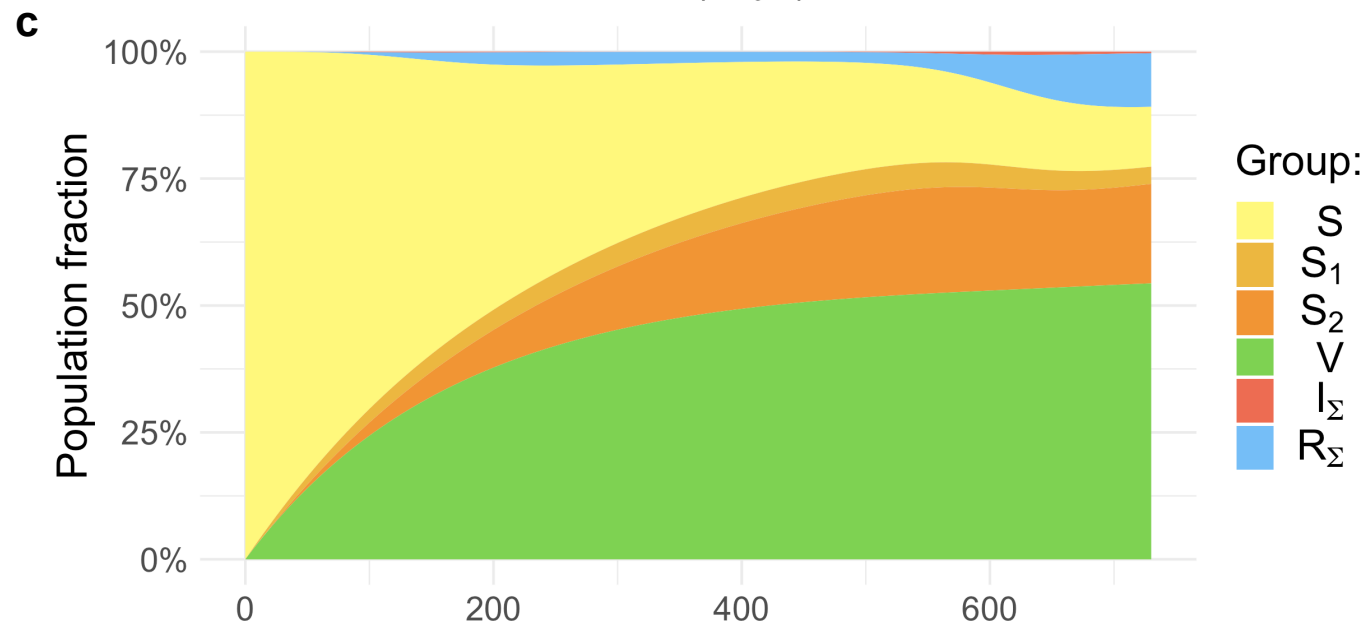
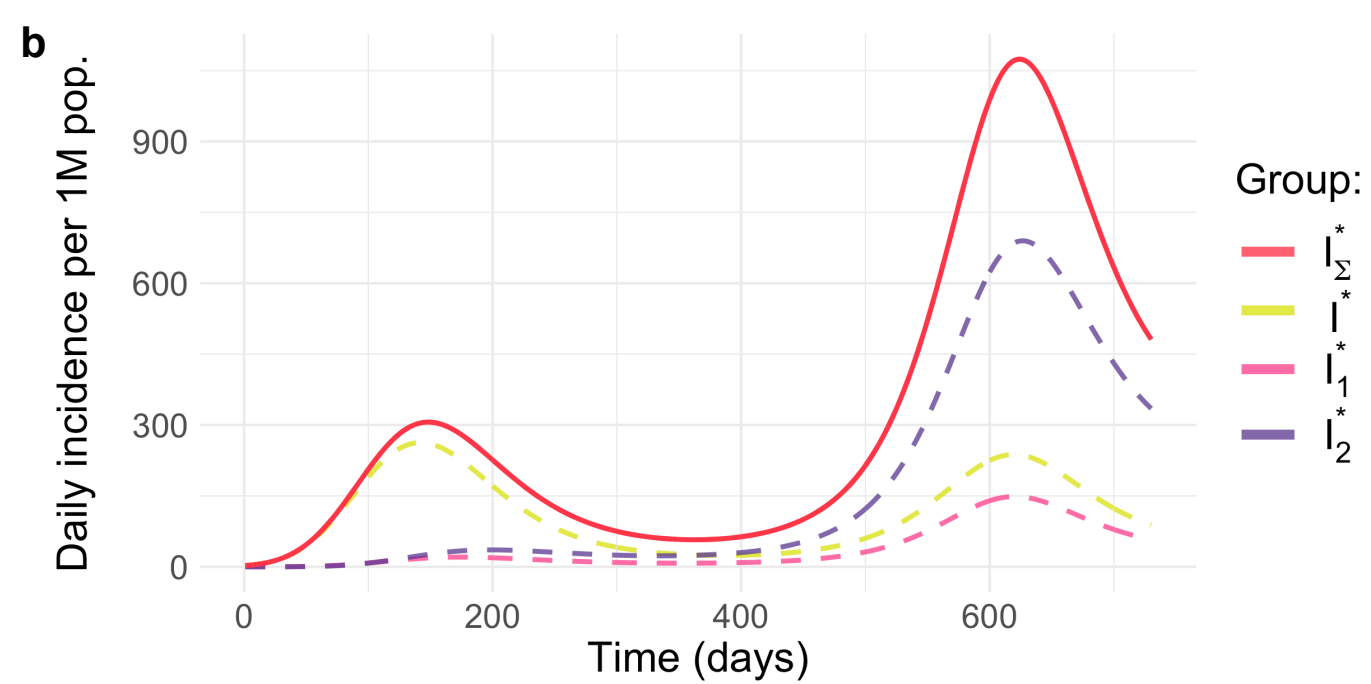
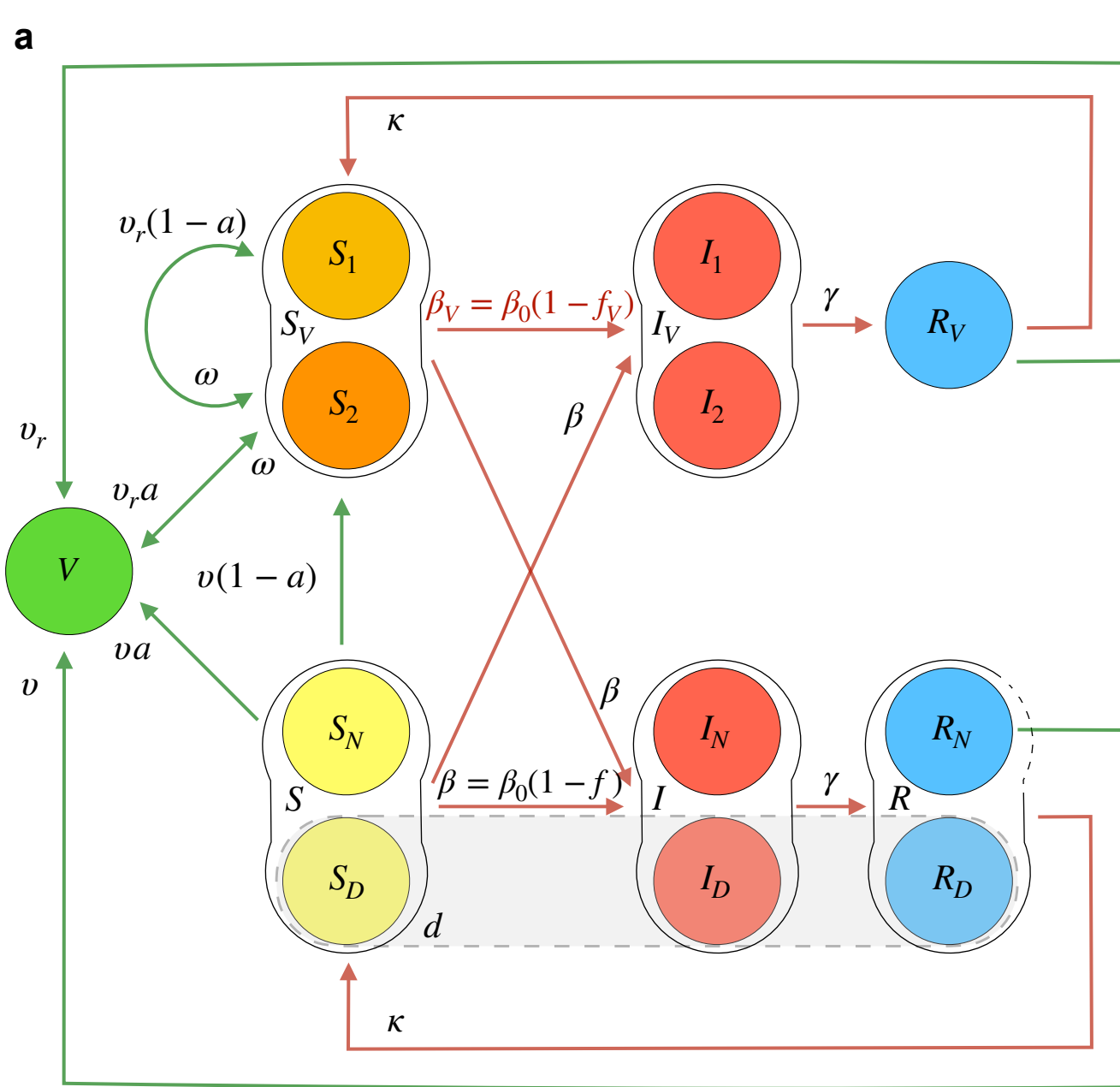
223 AG, KG, TK, and ES conceived the VAP-SIRS model - with input and feedback on the model
224 and results from TC, GG, MP, EP and MR. TK performed the stability analysis. KG implemented
225 model simulations and the Shiny application for visualizations. MB implemented the stability
226 analysis. SC, TC, EP, and MR performed literature search. ES supervised the study. All authors
227 wrote and provided critical feedback to the manuscript.

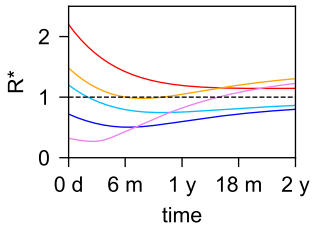
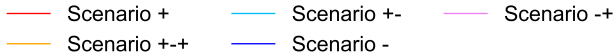
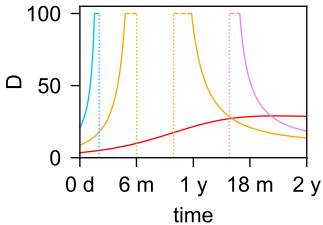
228 **Competing interests**

229 Other projects in the research lab of ES are co-funded by Merck Healthcare KGaA .

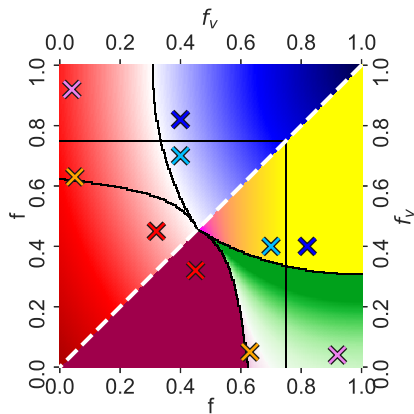
230 **Additional information**

231 Correspondence and requests for materials should be addressed to ES. Reprints and permissions
232 information is available at www.nature.com/reprints.

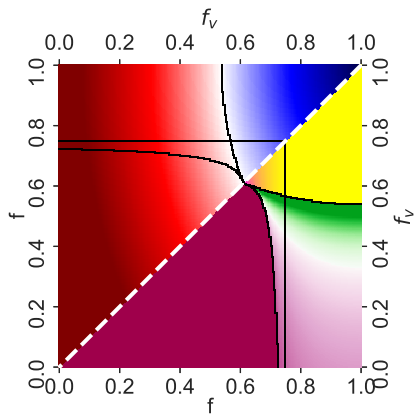


a**b**

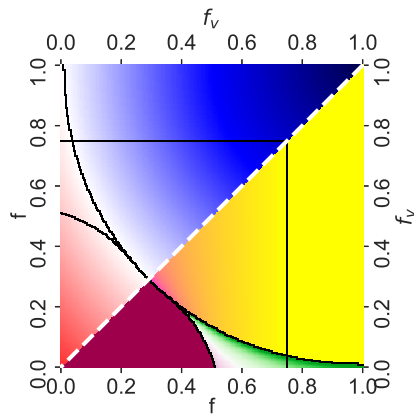
a $a = 0.9, \nu = 0.004, \omega = 0.002, d = 0.1$



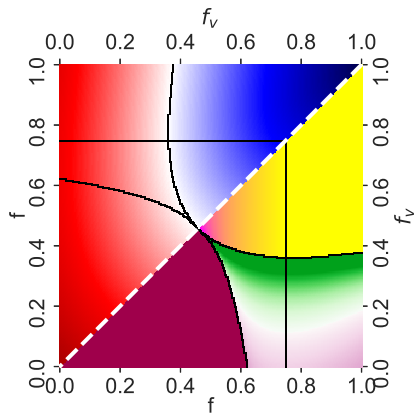
b change to reference: $a = 0.6$



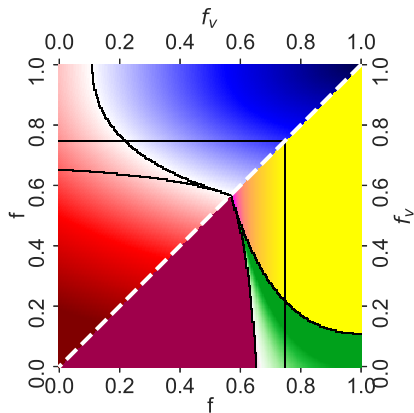
c change to reference: $\nu = 0.008$



d change to reference: pref mix



e change to reference: $d = 0.3$



f change to reference: $\omega = 0.005$

